Topology Preserving Digitization with FCC and BCC Grids

Peer Stelldinger[1] and Robin Strand[2]

[1] Cognitive Systems Group, University of Hamburg,
Vogt-Köln-Str. 30, D-22527 Hamburg, Germany
stelldinger@informatik.uni-hamburg.de
[2] Centre for Image Analysis, Uppsala University,
Lägerhyddsvägen 3, SE-75237 Uppsala, Sweden
robin@cb.uu.se

Abstract. In digitizing 3D objects one wants as much as possible object properties to be preserved in its digital reconstruction. One of the most fundamental properties is topology. Only recently a sampling theorem for cubic grids could be proved which guarantees topology preservation [1]. The drawback of this theorem is that it requires more complicated reconstruction methods than the direct representation with voxels. In this paper we show that face centered cubic (fcc) and body centered cubic (bcc) grids can be used as an alternative. The fcc and bcc voxel representations can directly be used for a topologically correct reconstruction. Moreover this is possible with coarser grid resolutions than in the case of a cubic grid. The new sampling theorems for fcc and bcc grids also give absolute bounds for the geometric error.

1 Introduction

In 3D image analysis one often has to deal with the huge amount of data of volumetric images. Using non-standard grids, like bcc and fcc grids for digitizing 3D objects is a very promising method in order to reduce the amount of data, since these grids have a very high packing density (i.e. the ratio between the volume of the largest ball completely enclosed in a voxel and the volume of the voxel itself) in comparison to cubic grids [2, 3]. The advantages of the bcc and fcc grids has led to various applications in very different areas, e.g. in fuzzy segmentation [4] and in computer graphics and data visualization, [2, 5, 6]. Also, image processing algorithms on which many applications rely have been developed for these grids, e.g. weighted distance transforms [7] and multiscale representation of images [8].

The question addressed in this paper is, if these grids can be used for topology preserving digitization and if they are advantageous regarding this problem relatively to the common cubic grid.

While first solutions to topology preserving digitization in 2D have already been published in 1982 [9,10], the 3D generalization remained unproved for over 20 years. In fact it is proved that topological changes can never be avoided if one uses the digital reconstruction on a cubic grid, i.e. the union of the voxels

whose sampling points lie inside the object [11]. At least connectivity and the number of the objects components could be reliably detected with the digital reconstruction, as shown in [12]. But this is not all the topological information. Only recently one of the authors showed together with Siqueira and Latecki that one can digitize 3D r-regular objects with a sufficiently dense sampling grid, such that the whole topological information is unchanged, if one uses not the digital reconstruction based on the voxels, but certain other reconstruction methods [1].

As we will show in this paper, the use of a sufficiently dense bcc or fcc grid leads to a topologically correct digital reconstruction, i.e. one does not need to use more complicated reconstruction methods. Moreover the grid density which is necessary for proving the preservation of topology is for both fcc and bcc grids smaller than for cubic grids, i.e. one needs much less sampling points in order to guarantee the right topology.

2 Preliminaries

The *(Euclidean) distance* between two points x and y in $\mathbb{R}^n$ is denoted by $d(x, y)$, and the *Hausdorff distance* $d_H(\cdot, \cdot)$ between two subsets of $\mathbb{R}^n$ is the maximal distance between each point of one set and the nearest point of the other. Let $A \subset \mathbb{R}^n$ and $B \subset \mathbb{R}^m$ be sets. A function $f : A \to B$ is called *homeomorphism* if it is bijective and both it and its inverse are continuous. If f is a homeomorphism, we say that A and B are *homeomorphic*. Let A, B be two subsets of $\mathbb{R}^3$. Then A homeomorphism $f : \mathbb{R}^3 \to \mathbb{R}^3$ such that $f(A) = B$ and $d(x, f(x)) \leq r$, for all $x \in \mathbb{R}^3$, is called an *r-homeomorphism* of A to B and we say that A and B are *r-homeomorphic*. A *Jordan curve* is a set $J \subset \mathbb{R}^n$ which is homeomorphic to a circle. Let A be any subset of $\mathbb{R}^3$. The *complement* of A is denoted by A^c. All points in A are *foreground* while the points in A^c are called *background*. The *open ball* in $\mathbb{R}^3$ of radius r and center c is the set $\mathcal{B}^0_r(c) = \{x \in \mathbb{R}^3 \mid d(x, c) < r\}$, and the *closed ball* in $\mathbb{R}^3$ of radius r and center c is the set $\overline{\mathcal{B}}_r(c) = \{x \in \mathbb{R}^3 \mid d(x, c) \leq r\}$. Whenever $c = (0, 0, 0)$, we write $\mathcal{B}^0_r$ and $\overline{\mathcal{B}}_r$. We say that A is *open* if, for each $x \in A$, there exists a positive number r such that $\mathcal{B}^0_r(x) \subset A$. We say that A is *closed* if its complement, A^c, is open. The *boundary* of A, denoted ∂A, consists of all points $x \in \mathbb{R}^3$ with the property that if B is any open set of $\mathbb{R}^3$ such that $x \in B$, then $B \cap A \neq \emptyset$ and $B \cap A^c \neq \emptyset$. We define $A^0 = A \setminus \partial A$ and $\overline{A} = A \cup \partial A$. Note that A^0 is open and $\overline{A}$ is closed, for any $A \subset \mathbb{R}^3$. Note also that $\mathcal{B}^0_r(c) = (\overline{\mathcal{B}}_r(c))^0$ and $\overline{\mathcal{B}}_r(c) = \overline{\mathcal{B}^0_r(c)}$. The *$r$-dilation* $A \oplus \mathcal{B}^0_r$ of a set A is the union of all open r-balls with center in A, and the *r-erosion* $A \ominus \mathcal{B}^0_r$ is the union of all center points of open r-balls lying inside of A. We say that an open ball $\mathcal{B}^0_r(c)$ is *tangent* to ∂A at a point $x \in \partial A$ if $\partial A \cap \partial \mathcal{B}^0_r(c) = \{x\}$ and $\partial A \cap \mathcal{B}^0_r(c) = \emptyset$. We say that an open ball $\mathcal{B}^0_r(c)$ is an *osculating open ball of radius r to ∂A at point* $x \in \partial A$ if $\mathcal{B}^0_r(c)$ is tangent to ∂A at x and either $\mathcal{B}^0_r(c) \subseteq A^0$ or $\mathcal{B}^0_r(c) \subseteq (A^c)^0$. Since all of the known topology preserving sampling theorems in 2D require the object to be r-regular [9–11], we will use the 3D generalization for our approach (refer to Fig. 1):

Definition 1. *A set $A \subset \mathbb{R}^3$ is called* r-regular *if, for each point $x \in \partial A$, there exist two osculating open balls of radius r to ∂A at x such that one lies entirely in A and the other lies entirely in A^c.*

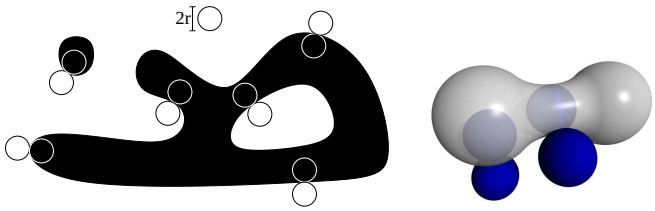

Fig. 1. For each boundary point of a 2D/3D r-regular set there exists an outside and an inside osculating open disc/ball of radius r.

Note, that the boundary of an r-regular set is a 2D manifold surface.

A countable set $S \subset \mathbb{R}^3$ of *sampling points* with $d_H(\mathbb{R}^3, S) \leq r'$ for some $r' \in \mathbb{R}_+$ such that $S \cap A$ is finite for each bounded set A, is called *r'-grid*. r' is called the covering radius. The *voxel* $\mathcal{V}_S(s)$ of a sampling point s is its Voronoi region, i.e. the set of all points lying at least as near to this point as to any other sampling point.

Given a translation vector t and a rotation matrix R in 3D, the *bcc* and *fcc* *r'-grids* are defined by $S := \{t + R \cdot \frac{2}{\sqrt{5}}(x_1, x_2, x_3) | x_1, x_2, x_3 \in \mathbb{Z}, x_1 \equiv x_2 \equiv x_3 (\mathrm{mod} 2)\}$ and $S := \{t + R \cdot (x_1, x_2, x_3) | x_1, x_2, x_3 \in \mathbb{Z}, x_1 + x_2 + x_3 \equiv 0 (\mathrm{mod} 2)\}$. Due to the scaling factor these grids are r'-grids. Note that the Hausdorff distance between a 3D object and an r'-grid is at most r', thus different sampling grids with the same covering radius lead to results with a geometrically comparable accuracy (see Fig. 10(2) to (4)). Note, that both bcc and fcc grids can be embedded in a cubic grid, as is illustrated in Fig. 2.

The intersection of $A \subseteq \mathbb{R}^3$ with S is called the *digitization* of A with S. The *digital reconstruction* of A with S is the union of all voxels belonging to the sampling points of the digitization. Two voxels are *face-adjacent* or *adjacent* if they share a face. They are *vertex-adjacent* if they intersect in exactly one point (this is not possible for bcc grids).

3 Digital Reconstruction of r-Regular Sets

Let $A \subset \mathbb{R}^3$ be an r-regular object, let S be a bcc or a fcc r'-grid, and consider the digital reconstruction $\hat{A}$ of A with respect to S. Assume that no sampling point of S lies on ∂A. This assumption is not a restriction, as if some sampling point lies on ∂A, there always exists an $\varepsilon > 0$ such that the ε-dilation $A \oplus \overline{\mathcal{B}}_\varepsilon$ is $(r - \varepsilon)$-regular with $r - \varepsilon > r'$, and $A \oplus \overline{\mathcal{B}}_\varepsilon$ has the same digital reconstruction as A, thus by updating r to the value of $r - \varepsilon$, the assumption is true.

In this section we will show that certain configurations of neighboring voxels in an fcc or a bcc grid can not occur in a sufficiently dense digitization of an

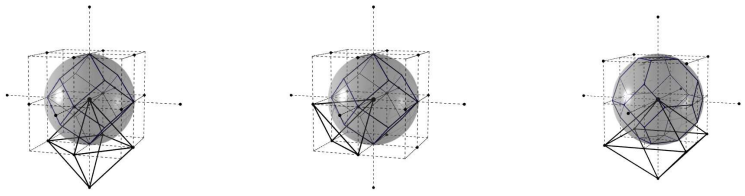

(a) (b) (c)

Fig. 2. Both fcc (a),(b) and bcc (c) grids can be embedded in cubic grids of higher resolution. The points are neighboring sampling points of the shown voxel of the fcc, respectively bcc grid, and the dashed lines show the cubic grid. The shown spheres have radius r'. The dual grid of an fcc r'-grid consists of octahedra (a) and tetrahedra (b). All line segments of them have length $\sqrt{2}r'$. The faces of both octahedra and tetrahedra are equilateral triangles. Based on the included cubic grid, a bcc r'-grid can be completely separated into octahedral configurations (c). Four of the line segments of the octahedra have length $\frac{4}{\sqrt{5}}r'$ and eight have length $2\sqrt{\frac{3}{5}}r'$. The faces of the octahedra are isosceles triangles with one angle of $2\arcsin\left(\frac{1}{\sqrt{3}}\right) \approx 70.53°$ and two angles of $\arccos\left(\frac{1}{\sqrt{3}}\right) \approx 54.74°$. Note that the fcc r'-grid is embedded in a cubic $\frac{\sqrt{3}}{2}$-grid, while the bcc r'-grid is embedded in a cubic $\sqrt{\frac{5}{3}}r'$-grid.

r-regular set and we will use this to show that the topology does not change during digitization. Therefore we need some definitions and lemmas about the local behavior of r-regular sets, which have already been introduced in [1]:

Definition 2. *Let x, y be two points in $\mathbb{R}^3$. Further let $s > d(x, y)$. Then, the intersection $P_s(x, y)$ of all closed s-balls containing x and y,*

$$P_s(x, y) = \bigcap \{\overline{\mathcal{B}}_s(v) \mid x, y \in \overline{\mathcal{B}}_s(v)\},$$

is called s-path region between x and y.

Now, let x, y, z be three points in $\mathbb{R}^3$, and assume that $s > \frac{1}{2}\max\{d(x, y), d(x, z), d(y, z)\}$. Then, the intersection $P_s(x, y, z)$ of all closed s-balls containing x, y and z,

$$P_s(x, y, z) = \bigcap \{\overline{\mathcal{B}}_s(v) \mid x, y, z \in \overline{\mathcal{B}}_s(v)\},$$

is called s-surface region between x, y and z.

A nonempty set B is called an r-simple-cut set *if it is the intersection of (a maybe infinite number of) closed balls with radii smaller than r.*

Lemma 1. *Let A be an r-regular set and x, y be two different points in A with $d(x, y) < 2r$. Further, let L be the straight line segment from x to y. Then, the function f mapping each point of L to the nearest point in A is well-defined, continuous and bijective, and the range of f is a simple path from x to y.*

Proof. Each point $L \cap A$ is its own nearest point in A. Since the intersection of surface normals of r-regular sets has a minimal distance of r to the surface [13], there exists for each point in $L \setminus A$ exactly one nearest point in ∂A because each

of these points has a distance smaller than r to the boundary. Thus f must be a continuous function since if f would not be continuous at some point, this point would have more than one nearest point in ∂A. Note that any point of L lies on the normal vector of ∂A in its nearest boundary point. Now suppose one point p of ∂A would be the nearest point to at least two different points l_1 and l_2 of L. Then l_1 and l_2 both lie on the normal of ∂A in p. This implies that any point in L including x and y lies on this normal. Since the normal vectors of length r of an r-regular set do not intersect, the distance between x and y has to be at least $2r$ which contradicts $d(x, y) < 2r$. Thus f is bijective. Since every bijective continuous function of a compact metric space is continuous in both directions, f must be a homeomorphism. This implies that the range is a simple path from x to y. □

Definition 3. *Let A be an r-regular set and x, y be two different points in A with $d(x, y) < 2r$. Further, let L be the straight line segment from x to y. Then, the range of the function f mapping each point of L to the nearest point in A is called the* direct path *from x to y regarding A.*

Lemma 2. *Let A be an r-regular set and x, y be two points both inside A or both outside A with $d(x, y) < 2r$. Then, $P_s(x, y)$ is a simple-cut set for any s with $\frac{1}{2} \cdot d(x, y) \leq s < r$, the direct path from x to y regarding A lies inside $A \cap P_s(x, y)$ and the direct path from x to y regarding $\overline{(A \ominus \overline{\mathcal{B}}_\varepsilon)^c}$ lies inside $\overline{A^c} \cap P_s(x, y)$ for a sufficiently small $\varepsilon > 0$.*

Proof. First, let $x, y \in A$. Since $d(x, y) < 2r$, $P_s(x, y)$ is a simple cut set for any s with $\frac{1}{2} \cdot d(x, y) \leq s < r$. Now, suppose there exists a point p on the direct path lying outside of $P_s(x, y)$. Then the outside osculating open r-ball of A in p must cover either x or y which implies that they cannot lie on ∂A or inside A. Thus, the direct path has to be inside $P_s(x, y)$. If $x, y \in A^c$ the analog is true by looking at the $(r - \varepsilon)$-regular set $\overline{(A \oplus \overline{\mathcal{B}}_\varepsilon)^c}$ for a sufficiently small $\varepsilon > 0$, since there alway exists an ε such that x and y remain outside $A \oplus \overline{\mathcal{B}}_\varepsilon$ and $s < (r - \varepsilon)$. □

Lemma 3. *Let A be an r-regular set and let B be an s-simple-cut set with $s < r$. Further, let $B^0 \cap A^0 \neq \emptyset$ and $B \cap A^c \neq \emptyset$. Then, the intersection of the boundaries of A and B, $\partial A \cap \partial B$, is a Jordan curve.*

Proof. Let c_1 and c_2 be two arbitrary points in $B \cap A$ and let P be the direct path from c_1 to c_2. Then P lies inside of B due to lemma 2 and $P_s(c_1, c_2) \subset B$. This implies that $B \cap A$ must be one connected component.

Now, consider the two points c_1 and c_2 lying in $B \cap A^c$. Then the direct path does not necessarily lie in A^c since this set is open, but in $\overline{A^c}$. Thus for any open superset of the intersection of all r-balls containing c_1 and c_2 there exists a path from c_1 to c_2 inside this superset having a minimal distance to the direct path in $\overline{A^c}$. $(B \cap A^c)^0$ is such a superset, since $\partial(B \cap A^c)$ intersects the intersection only in c_1 and c_2.

Thus both $B \cap A$ and $B \cap A^c$ have to be one component and thus the intersection of the boundaries, $I = \partial A \cap \partial B$, must also be one component.

It remains to be shown that I is a Jordan curve. Since I separates ∂B in one part inside of A and one part outside of A, it is a Jordan curve if and only if there exists no point where B and A meet tangentially. Such a point would imply that either the inside or the outside osculating ball of A at this point covers B. Both cases are impossible since then $B^0 \cap A^0 = \emptyset$ or $B \cap A^c = \emptyset$. Thus, $\partial A \cap \partial B$ is a Jordan curve. □

Definition 4. *Let A be an r-regular set and let x, y, z be three arbitrary points inside of $A^0 \oplus \overline{\mathcal{B}}_r$. Then, the* inner surface patch $I_s(x, y, z)$ *of x, y, z regarding A is the set defined by mapping each point of the triangle T spanned by points x, y, z to itself if it lies inside of A and mapping it to the nearest boundary point in ∂A otherwise.*

Now, let x, y, z be three arbitrary points inside of $A^c \oplus \overline{\mathcal{B}}_r$. Then the outer surface patch $O_s(x, y, z)$ *of x, y, z regarding A is the set defined by mapping each point of the triangle T between the points to itself if it lies inside of $\overline{(A \oplus \overline{\mathcal{B}}_\varepsilon)^c}$ and mapping them to the nearest boundary point $\partial\overline{(A \oplus \overline{\mathcal{B}}_\varepsilon)^c}$ otherwise, with ε being half the minimal distance from the sampling points in A^c to ∂A.*

Lemma 4. *Let A be an r-regular set and x, y, z be three points inside A with* $\max\{d(x, y), d(x, z),$
$d(y, z)\} < 2r$. *Then $P_s(x, y, z)$ is a simple cut set for any s with $\frac{1}{2} \cdot d(x, y) \leq s < r$ and the inner surface patch is homeomorphic to a disc, lies inside $A \cap P_s(x, y)$ and is bounded by three paths, one going from x to y inside of $P_s(x, y, z) \cap P_s(x, y)$, another going from y to z inside of $P_s(x, y, z) \cap P_s(y, z)$ and the third going from z to x inside of $P_s(x, y, z) \cap P_s(z, x)$. The analog is true for x, y, z lying outside of A and the outer surface patch.*

Proof. The mapping used in definition 4 is a direct generalization of the mapping in definition 3 and it is a homeomorphism for the same reasons if x, y, z lie inside A and $\max\{d(x, y), d(x, z), d(y, z)\} < 2r$. Its boundaries are equal to the direct paths between each two of the three points. If x, y, z lie outside of A the proof is analog. □

In the next two subsections we will use these properties of r-regular objects for our proofs of the topology preservation. Therefore let s be an arbitrary but fixed number with $r' < s < r - \varepsilon$.

3.1 Digital Reconstruction on FCC Grids

Let us have a closer look at fcc grids. The Delaunay grid separates the space $\mathbb{R}^3$ into octahedra and tetrahedra due to the two types of voxel corners in an fcc grid with 6 respectively 4 neighboring voxels (see Fig. 2(a) and (b)). The digital reconstruction inside an octahedron respectively tetrahedron is totally determined by the sampling points at its vertexes. By our above assumption,

each vertex of such an octahedron is either inside (i.e., a foreground point) or outside (i.e., a background point) A. So, there are at most $2^6 = 64$ distinct configurations for a octahedron and $2^4 = 16$ configurations for a tetrahedron with respect to the binary "status" of the vertices. However, up to rotational symmetry, reflectional symmetry, and complementarity (switching foreground and background points), these configurations are equivalent to the 6 canonical configurations for the octahedron and the 3 configurations for the tetrahedron shown in Fig. 3. In the following we will show that case 4 of the 6 octahedron

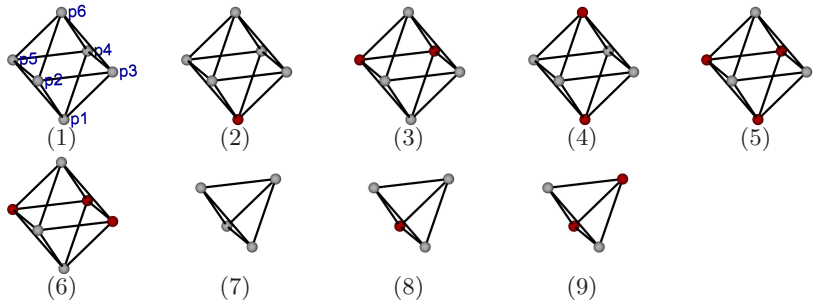

Fig. 3. There are 64+16 distinct configurations in an fcc grid for neighboring sampling points that are either inside or outside a digitized set. However, up to rotational symmetry, reflectional symmetry, and complementarity (switching foreground and backgroud points), these 80 configurations are equivalent to the above 9 canonical configurations.

configurations can not occur if one digitizes an r-regular object with a sufficiently dense fcc grid. The problem of topology preserving digitization is that in case of configuration 4 a non-manifold surface is reconstructed, which can not be guaranteed to be topologically equivalent to the surface of the original object. This can be avoided by using a sufficiently dense sampling grid for digitizing an r-regular object, as shown by the following theorem:

Theorem 1. *Configuration 4 in Fig. 3 cannot occur in the digital reconstruction of an r-regular object with an fcc r'-grid with $\sqrt{2}r' < r$.*

Proof. In the following let the dark sampling points in Fig. 3 be in the foreground and the white sampling points in the background. Further, let the sampling points $p_1, p_2, \ldots p_6$ of an octahedron be numbered as shown in Fig. 3(a).

Suppose to the contrary, configuration 4 occurs in the digital reconstruction of an r-regular object A. Since the distance from p_1 to p_6 is $2r'$ and thus smaller than $2r$, there exists a foreground path between these points lying completely inside $P_s(p_1, p_6)$.

On the other side, the three background points p_2, p_3, p_4 have each a distance being smaller than $2r$. Thus, due to Lemma 4, there exists an outer surface patch between them. This patch lies inside $P_s(p_2, p_3, p_4)$ with its surface boundary lying inside the union of $P_s(p_2, p_3)$, $P_s(p_2, p_4)$ and $P_s(p_3, p_4)$. Analogously there exists a outer surface patch between the three background points p_2, p_4, p_5 with its boundary in $P_s(p_2, p_4)$, $P_s(p_2, p_5)$ and $P_s(p_4, p_5)$. Due their definition, the two

outer surface patches have the boundary part inside $P_s(p_2, p_4)$ in common such that together they form a surface patch between the four points p_2, p_3, p_4, p_5. Fig. 4(b) and (c) show that $P_s(p_1, p_6)$ goes through this surface patch without intersecting the bounding r-path regions for $\sqrt{2}r' = r$ (Obviously this is also true for smaller r'). Since both p_1 and p_6 lie outside $P_s(p_2, p_3, p_4) \cup P_s(p_2, p_4, p_5)$, the path from p_1 to p_6 must go through the combined surface patch and thus there has to exist a point lying both in A and A^c. It follows that case 4 cannot occur in the digital reconstruction of an r-regular object if $\sqrt{2}r' < r$. □

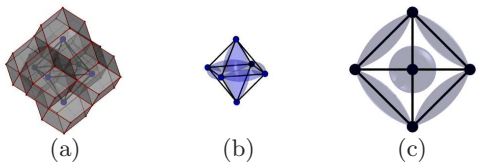

Fig. 4. Case 4 is impossible in dense digitizations (a) of r-regular objects with an fcc grid, since the path region crosses the outer surface region (b) and topview (c).

We have seen that case 4 is impossible if we use a sufficiently dense sampling grid. As one can see, in the remaining cases the intersection of one of the octahedra and the boundary of the digital reconstruction is always either empty (case 1) or homeomorphic to a disc, such that the octahedron is divided into an inner and an outer part, both homeomorphic to a ball (cases 2,3,5 and 6), see Fig. 5. This fact allows us to derive the following sampling theorem: The above theorem

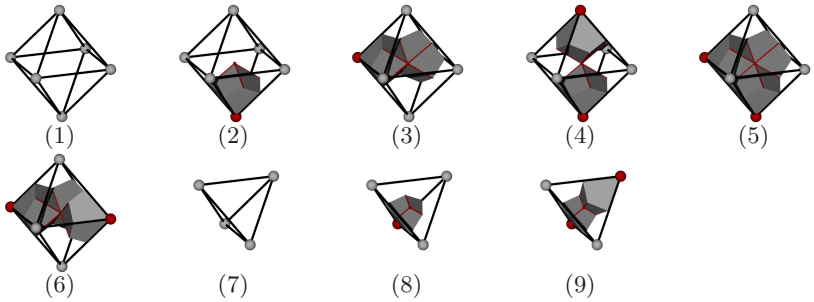

Fig. 5. Local reconstructions with the fcc grid inside the octahedra and tetrahedra. Note that for all cases except of cases 1, 4 and 7 the surface of the reconstruction inside the octahedra and tetrahedra is homeomorphic to a disc.

allows us to derive a sampling theorem for fcc grids, since it implies that the surface of the reconstruction is locally disc-shaped, which is also the case for the original r-regular object.

Theorem 2. *Let A be an r-regular object and S be an fcc r'-grid with $\sqrt{2}r' < r$. Then the digital reconstruction is $2r' + \varepsilon$-homeomorphic to A.*

Proof. Due to Theorem 1, the only cases which can occur in the digitization of an r regular object with an fcc r'-grid with $\sqrt{2}r' < r$ are cases 1 to 9 except of case 4.

Now consider a configuration of case 2,3,5 or 6 and let O denote the octahedron defined by the six sampling points. In these cases the intersection of ∂O and the boundary of the digital reconstruction is a Jordan curve (see Fig. 5). The same is true for cases 8 and 9 in the tetrahedron. Now each face F_i of the octahedron respectively tetrahedron is a triangle with its corner points having a distance of $\sqrt{2}r'$, i.e. smaller than $2r$. We define a new surface patch for such a triangle between three sampling points in the following way:

If all three sampling points p_1, p_2, p_3 lie inside of A, we take the inner surface patch. Analogously if all three sampling points lie outside of A, we take the outer surface patch.

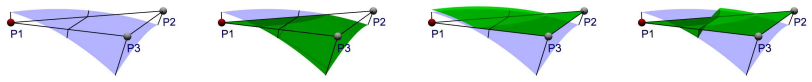

(a) (b) (c) (d)

Fig. 6. In order to construct a surface between three sampling points being not all in the foreground (a), we combine the inner (b) and the outer surface patch (c) such that the result (d) is cut by ∂A into exactly two parts.

If only one sampling point p_1 lies inside of A, we use the mapping of the inner surface patch for each point lying inside the smaller triangle $\triangle(p_1, \frac{p_1+p_2}{2}, \frac{p_1+p_3}{2})$ and the mapping of the outer surface patch otherwise, see Fig. 6 for an illustration. In order to get a connected surface, we further add the straight line connections between the inner and the outer surface patch for any point lying on the straight line from $\frac{p_1+p_2}{2}$ to $\frac{p_1+p_3}{2}$. If one sampling point lies outside and the other two inside of A, we define the mapping analogously.

This leads to a surface patch between the three points which is always homeomorphic to a disc. Furthermore, since any of the added straight line connections follows a normal of ∂A and thus cuts ∂A exactly once, the intersection of the surface patch with ∂A is a simple curve.

By combining the surface patches of the octahedron respectively tetrahedron faces we get a surface homeomorphic to the octahedron respectively tetrahedron surface intersecting ∂A in a Jordan curve.

In order to guarantee that the new surface patches can be combined without topological errors, we have to show that they can only intersect in their boundaries. This is true if any two path regions can only intersect in common sampling points. Since any angle α of any of the equilateral octahedron or tetrahedron triangles is $60°$, we only have to ensure that the opening angle β of the cigar shaped path regions is smaller than $60°$. One can easily show that $\beta = 2 \arcsin\left(\frac{l}{2r}\right)$ with $l = \sqrt{2}r'$ being the distance between the two sampling points, and thus $\beta < 60°$ for $\sqrt{2}r' < r$.

If we have a octahedron of case 1 or a tetrahedron of case 7, we also can take the above surface patch construction, since it only consists of triangles lying completely inside respectively completely outside of A and thus the surface patches are well-defined. The resulting combined surface does not intersect ∂A at all.

Thus we have partitioned the whole space into deformed octahedral and tetrahedral regions separated by the new surface patches. The original object is homeomorphic to the result of the digital reconstruction inside each of the regarded regions. The combination of the local homeomorphisms (each being a $(2r' + \varepsilon)$-homeomorphism) leads to a global r-homeomorphism from A to the reconstructed set. □

The above theorem states that an r-regular object can be reconstructed without any change in the topological information by using an fcc r'-grid with $\sqrt{2}r' < r$. This means that one only needs 4 sampling points per cube of sidelength $2r'$ and thus only a bit more than $\sqrt{2}$ sampling points per cube of sidelength r. This is much better than using a cubical sampling grid: The sampling theorem for cube grids derived in [1] needs $2r' < r$ and thus more than 8 sampling points per cube of sidelength r in order to guarantee topology preservation. This is more than 5.6 times the number of sampling points needed with an fcc-grid! See Fig. 10(5) to (7) for an example.

In addition to that topology preserving digitization on a cubic grid needs more complicated reconstruction methods than the digital reconstruction, as shown in [11] and [1] – whereas by using an fcc grid one can directly use the digital reconstruction.

There is another interesting implication of the above sampling theorem: Given an r-regular object we have to use a sampling grid with $2r' < r$ if we want to guarantee topology preservation and if we use cubic sampling grids. Now we make use of the fact that one can construct an fcc $\frac{2}{\sqrt{3}}r'$-grid by removing every second sampling point in a cubic r'-grid. Then we only need $\sqrt{2} \cdot \frac{2}{\sqrt{3}}r' < r$. Thus by throwing away half of the sampling points of the cubic grid and using the digital reconstruction on the resulting fcc grid, we can derive the correct topology at resolutions where this is not possible by reconstructing directly on the cubic grid, as can be seen in Fig. 10(8) to (13).

3.2 Digital Reconstruction on BCC Grids

In this subsection we will derive an analogous result to the ones of the last section for bcc grids. The voxels of a bcc grid are truncated octahedra having eight hexagonal and six square faces (see Fig. 2(c)). Thus two face-adjacent bcc voxels share either a hexagonal face or a square face.

Similarily to the fcc grid, we can partition the space $\mathbb{R}^3$ into octahedra based on the bcc grid. These octahedra are not directly given by the Delaunay grid. They are instead each a union of 4 tetrahedra of the Delaunay grid and they can be defined as follows: The bcc grid $S = \{\frac{2}{\sqrt{5}}(x_1, x_2, x_3) | x_1, x_2, x_3 \in \mathbb{Z}, x_1 \equiv$

$x_2 \equiv x_3 (\mathrm{mod} 2)\}$ contains the cubic grid $S' = \{\frac{4}{\sqrt{5}}(x_1, x_2, x_3) | x_1, x_2, x_3 \in \mathbb{Z}\}$, such that the remaining sampling points of $S \setminus S'$ are the center points of the dual cubes in S'. Now we can define for each face of a dual cube an octahedron by connecting its four corner points with the center points of the two adjacent dual cubes (see Fig. 2(c)). Each octahedron connects two bcc voxels sharing a square face and their common four neighbors (see Fig. 8(a)). The same partition into octahedra is used in [6] for building a polygonal surface reconstruction.

In contrast to the regular octahedra of the fcc grids, these octahedra are not regular, but square dipyramids with baselength $\frac{4}{\sqrt{5}}$ and pyramid height $\frac{2}{\sqrt{5}}$. Thus not 6 but 10 different canonical configurations have to be distinguished, see Fig. 7. Analogously to case 4 of the fcc grid we will now show that cases 4a

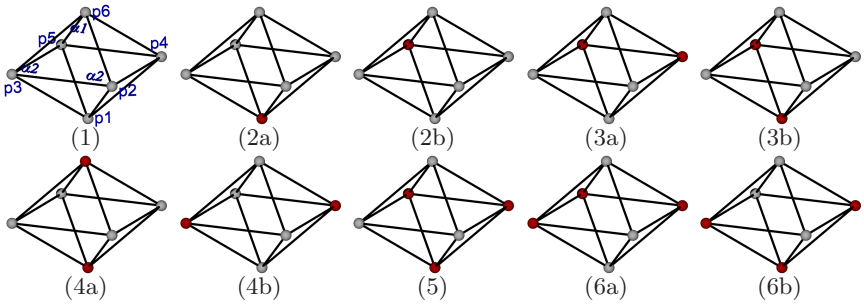

Fig. 7. There are 64 distinct configurations in a bcc grid for sampling points in an octahedron. However, up to rotational symmetry, reflectional symmetry, and complementarity (switching foreground and backgroud points), these 64 configurations are equivalent to the above 10 canonical configurations.

and 4b can not occur if one digitizes an r-regular object with a sufficiently dense bcc grid.

Theorem 3. *Configuration 4a and 4b in Fig. 7 cannot occur in the digital reconstruction of an r-regular object with a bcc r'-grid with $\sqrt{\frac{33}{10}} r' < r$.*

Proof. In the following let the dark sampling points in Fig. 7 be in the foreground and the white sampling points in the background. Further, let the sampling points $p_1, p_2, \ldots p_6$ be numbered as shown in Fig. 7(a).

Suppose configuration 4a occurs in the digital reconstruction of an r-regular object A. Since the distance from p_1 to p_6 is $\frac{4}{\sqrt{5}} r'$ and thus smaller than $2r$, there exists a foreground path between these points lying completely inside $P_s(p_1, p_6)$.

Analogously to the proof for the fcc grid, there exists a surface patch between the four points p_2, p_3, p_4, p_5, since their pairwise distance is at most $4\frac{\sqrt{2}}{\sqrt{5}} r' < 2r$. Fig. 8(b) and (c) show that $P_s(p_1, p_6)$ goes through this surface patch without intersecting the bounding r-path regions for $\sqrt{\frac{33}{10}} r' = r$ (Obviously this is also true for smaller r'). Since both p_1 and p_6 lie outside $P_s(p_2, p_3, p_4) \cup P_s(p_2, p_4, p_5)$, the path from p_1 to p_6 must go through the combined surface patch and thus there has to exist a point lying both in A and A^c.

Now suppose configuration 4b occurs in the digital reconstruction of an r-regular object A. Then the distance from p_2 to p_4 is $4\frac{\sqrt{2}}{\sqrt{5}}r'$ and thus smaller than $2r$, such that there exists a foreground path between these points lying completely inside $P_s(p_2, p_4)$.

In this case there can be constructed a surface patch between the four points p_1, p_3, p_5, p_6, since their pairwise distance is at most $4\frac{\sqrt{2}}{\sqrt{5}}r' < 2r$. Fig. 8(d) and (e) show that $P_s(p_2, p_4)$ goes through this surface patch without intersecting the bounding r-path regions for $\sqrt{\frac{33}{10}}r' = r$ (Obviously this is also true for smaller r'). Since both p_2 and p_4 lie outside $P_s(p_1, p_3, p_5) \cup P_s(p_3, p_5, p_6)$, the path from p_2 to p_4 must go through the combined surface patch and thus there has to exist a point lying both in A and A^c.

It follows that both cases 4a and 4b cannot occur in the digital reconstruction of an r-regular object if $\sqrt{\frac{33}{10}}r' < r$. □

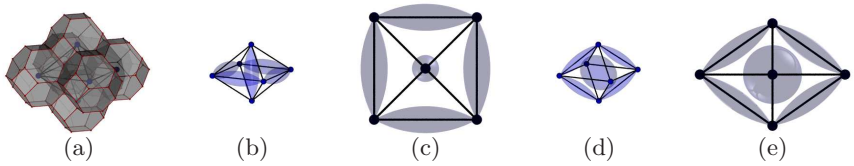

Fig. 8. Cases 4a (see (b) and (c)) and 4b (see (d) and (e)) are impossible in dense digitizations (a) of r-regular objects with a bcc grid.

We have seen that cases 4a and 4b are impossible if we use a sufficiently dense sampling grid. Fig. 9 illustrates that again in any of the remaining cases the boundary of the digital reconstruction intersects the octahedron in a simple surface, being homeomorphic to a disc, such that we can derive the following sampling theorem for bcc grids:

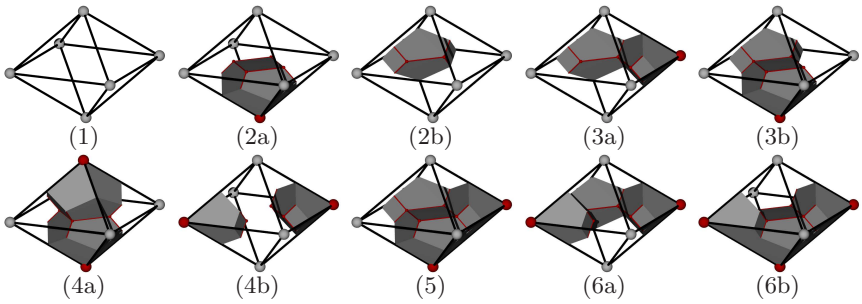

Fig. 9. Local reconstructions with the bcc grid inside the octahedra. Note that for all cases except of cases 1, 4a and 4b the surface of the reconstruction inside the octahedra is homeomorphic to a disc.

Theorem 4. *Let A be an r-regular object and S be a bcc r'-grid with $\sqrt{33/10}r' < r$. Then the digital reconstruction is $4\sqrt{2/5}r' + \varepsilon$-homeomorphic to A.*

Proof. Due to Theorem 3, cases 4a and 4b can not occur in the digitization of an r regular object with a bcc r'-grid with $\sqrt{33/10}r' < r$.

Now consider a configuration of one of the other cases except of case 1 and let O denote the octahedron defined by the six sampling points. In these cases the intersection of ∂O and the boundary of the digital reconstruction is a Jordan curve (see Fig. 9). Now each face F_i of the octahedron is a triangle with its corner points having a distance smaller than $2r$. We define a new surface patch for such a triangle between three sampling points in the same way as in Theorem 2.

Again, by combining the surface patches of the octahedron faces we get a surface homeomorphic to the octahedron surface intersecting ∂A in a Jordan curve.

In order to guarantee that the new surface patches can be combined without topological errors, we have to show that they can only intersect in their boundaries. This is true if any two path regions can only intersect in common sampling points. There exist two different angles $\alpha_1 = \arccos(1/3)$ and $\alpha_2 = 2\arcsin(1/\sqrt{3})$ in the corners of the octahedron triangles (see Fig. 7(a)). In both cases we have to ensure that these angles are bigger than the sum of the opening angles of the two corresponding path regions. While α_1 is between a triangle side of length $l_1 = 4/\sqrt{5} \cdot r'$ and a triangle side of length $l_2 = 2\sqrt{3/5}r'$, the angle α_2 is between two triangle sides of length l_2. Thus the two inequalities $\arcsin(l_1/2) + \arcsin(l_2/2) < \alpha_1$ and $2\arcsin(l_2/2) < \alpha_2$ have to be true, which is the case for $\sqrt{33/10}r' < r$.

Analogously to the proof of Theorem 2 it follows the existence of a homeomorphism from A to its digital reconstruction. This homeomorphism is a $4\sqrt{2/5}r' + \varepsilon$-homeomorphism, since $4\sqrt{2/5}r'$ is the maximal diameter of the octahedra. □

Thus not only fcc grids but also bcc grids can directly be used to reconstruct an r-regular object without any change in the topological information. In case of bcc grids one only needs 2 sampling points per cube of sidelength $4/\sqrt{5} \cdot r'$ and thus only a bit more than $\frac{33}{64}\sqrt{33/2} \approx 2.09$ sampling points per cube of sidelength r. This is 3.8 times better than a cubic grid, although it is not as good as an fcc grid.

4 Conclusions

We have analysed the problems of topology preservation during digitization of r-regular objects in 3D with fcc and bcc grids. We showed that with a sufficient sampling density both fcc and bcc grids directly lead to a topology preserving reconstruction, which is not the case for cubic grids as shown in [1], where one needs more complicated reconstruction methods. Thus we derived the first sampling theorem for topology preserving digitization with non-standard grids in 3D.

Both fcc and bcc grids outperform cubic grids in the sense that (1) less sampling points are needed and (2) a bigger covering radius of the sampling grid is allowed if one wants to guarantee the correct topology of the digitized object.

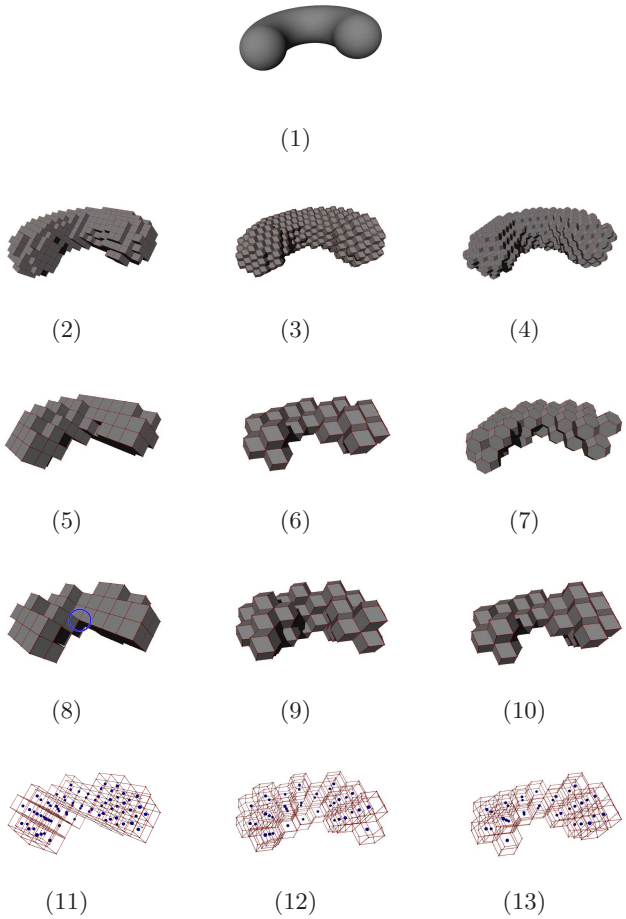

Fig. 10. Digitization of an r-regular object (1) with different r'-grids. Second row: Digital reconstruction with cubic (2), fcc (3) and bcc (4) r'-grid with $4r' = r$. As one can see, the quality of the reconstructions seems to be comparable for different grid types with the same r', while a different number of voxels is needed (972 voxels in (2), 774 voxels in (3) and 537 voxels in (4). Third row: Digital reconstruction with r' chosen near the critical values of the different grid types, i.e. $2r' = r - \varepsilon$ for the cubic grid (5), $\sqrt{2}r' = r - \varepsilon$ for the fcc grid (6) and $\sqrt{\frac{33}{10}}r' = r - \varepsilon$ for the bcc grid (7). For this example the topologically correct digital reconstruction needs 125 voxels in (5), 30 voxels in (6) and 43 voxels in (7). Fourth and fifth row: Digital reconstruction based on a cubic r'-grid with $1.5r' = r$. This resolution is not enough to guarantee topology preservation on cubic grids, as can be seen in the marked region in (8), but it allows topology preserving digitization on the two fcc subgrids (9) and (10). As can be seen in (11), (12) and (13), the sampling points of (8) are divided into two disjunct subsets of sampling points in fcc grid order.

We got better results for the fcc grid than for the bcc one. We even showed that at certain resolutions, where a cubic grid does not guarantee topology preservation, one can remove half of the sampling points from the cubic grid such that one gets an fcc grid with a resolution which is enough to reconstruct the topology!

Acknowledgment

We thank Prof. Gunilla Borgefors for valuable comments and suggestions.

References

1. P. Stelldinger and L.J. Latecki. 3D Object Digitization with Topological and Geometric Guarantees. In *University Hamburg, Computer Science Department, Technical Report FBI-HH-M-334/05*, 2005.
2. Thomas Theußl, Torsten Möller, and Meister Eduard Gröller. Optimal regular volume sampling. In *VIS '01: Proceedings of the conference on Visualization '01*, pages 91–98, Washington, DC, USA, 2001. IEEE Computer Society.
3. Luis Ibanez, Chafiaa Hamitouche, and Christian Roux. Determination of discrete sampling grids with optimal topological and spectral properties. In *Proceedings of* 6^{th} *Conference on Discrete Geometry for Computer Imagery, Lyon, France*, pages 181–192, 1996.
4. B. M. Carvalho, E. Gardu no, and G. T. Herman. Multiseeded fuzzy segmentation on the face centered cubic grid. In Springer-Verlag Ltd., editor, *Proceedings econd International Conference on Advances in Pattern Recognition ICAPR 2001*. ICAPR, Pattern Analysis and Applications journal.
5. Alois Dornhofer. A discrete fourier transform pair for arbitrary sampling geometries with applications to frequency domain volume rendering on the body-centered cubic lattice. Master's thesis, Vienna University of Technology, 2003.
6. Hamish Carr, Thomas Theußl, and Torsten Möller. Isosurfaces on optimal regular samples. In *VISSYM '03: Proceedings of the symposium on Data visualisation 2003*, pages 39–48. Eurographics Association, 2003.
7. Robin Strand and Gunilla Borgefors. Distance transforms for three-dimensional grids with non-cubic voxels. *Computer Vision and Image Understanding*, 100(3):294–311, dec 2005.
8. Robin Strand and Gunilla Borgefors. Resolution pyramids on the fcc and bcc grids. In Eric Andres, Guillaume Damiand, and Pascal Lienhardt, editors, *Discrete Geometry for Computer Imagery, 12th International Conference, DGCI 2005, Poitiers, France, April 13-15, 2005, Proceedings*, volume 3429 of *Lecture Notes in Computer Science*, pages 68–78. Springer, 2005.
9. T. Pavlidis. *Algorithms for Graphics and Image Processing*. Computer Science Press, 1982.
10. J. Serra. *Image Analysis and Mathematical Morphology*. Academic Press, 1982.
11. P. Stelldinger and U. Köthe. Towards a General Sampling Theory for Shape Preservation. *Image and Vision Computing Journal, Special Issue on Discrete Geometry for Computer Imagery*, 23(2):237–248, 2005.
12. P. Stelldinger. Digitization of Non-regular Shapes in Arbitrary Dimensions. *Submitted*.
13. L.J. Latecki, C. Conrad, and A. Gross. Preserving Topology by a Digitization Process. *Journal of Mathematical Imaging and Vision*, 8:131–159, 1998.